



Publication Year	2015
Acceptance in OA	2021-02-23T11:10:49Z
Title	The effect of diamagnetic drift on motion of the dayside magnetopause reconnection line
Authors	Trenchi, L., MARCUCCI, Maria Federica, Fear, R. C.
Publisher's version (DOI)	10.1002/2015GL065213
Handle	http://hdl.handle.net/20.500.12386/30551
Journal	GEOPHYSICAL RESEARCH LETTERS
Volume	42

**₁ The effect of diamagnetic drift on motion of the
₂ dayside magnetopause reconnection line**

L. Trenchi¹, M. F. Marcucci² and R. C. Fear¹

¹School of Physics and Astronomy,
University of Southampton, Southampton,
UK.

²INAF - Istituto di Astrofisica e
Planetologia Spaziali, Rome, Italy.

3 Magnetic reconnection at the magnetopause occurs with a large density
4 asymmetry and for a large range of magnetic shears. In these conditions, a
5 motion of the X-line has been predicted in the direction of the electron dia-
6 magnetic drift. When this motion is super-Alfvenic, reconnection should be
7 suppressed. We analysed a large dataset of Double Star TC-1 dayside mag-
8 netopause crossings, which includes reconnection and non-reconnection events.
9 Moreover, it also includes several events during which TC-1 is near the X-
10 line. With these close events we verified the diamagnetic suppression con-
11 dition with local observations near the X-line. Moreover, with the same close
12 events we also studied the motion of the X-line along the magnetopause. It
13 is found that, when reconnection is not suppressed, the X-line moves north-
14 ward or southward according to the orientation of the guide-field, which is
15 related to the interplanetary magnetic field B_Y component, in agreement with
16 the diamagnetic drift.

1. Introduction

17 Magnetic reconnection between the interplanetary magnetic field (IMF) and the geo-
 18 magnetic field is the main process that allows the transfer of solar wind mass, energy,
 19 and momentum into the Earth's magnetosphere. One of the most important controlling
 20 factors for magnetic reconnection at the magnetopause is the orientation of the IMF; for
 21 pure northward IMF antiparallel reconnection occurs at the high-latitude magnetopause
 22 poleward of the cusps; when the IMF is southward and/or has a large B_Y component,
 23 reconnection occurs at the dayside equatorial magnetopause. In this region several ob-
 24 servations have shown that the orientation of the X-line is related to the sign of the B_Y
 25 component, as predicted by the component merging model [Sonnerup, 1974; Gonzales &
 26 Mozer, 1974]. It is found that reconnection at the dayside magnetopause can occur also
 27 when the local magnetic shear angle is quite low (90° or less), i.e. in presence of a strong
 28 guide field [Scurry & Russell, 1994; Phan & Paschmann, 1996; Trenchi et al., 2008].

29 In these low shear conditions, according to the simulations of Swisdak et al. [2003] the
 30 X-line should experience a motion along the magnetopause due to the diamagnetic drift
 31 of ions and electrons. If this X-line motion exceeds the local Alfvén speed, reconnection is
 32 suppressed. Swisdak et al. [2010] proposed that reconnection is suppressed based on the
 33 local conditions at the X-line, if:

$$\Delta\beta > 2\frac{L_p}{d_i}\tan\left(\frac{\theta}{2}\right) \quad (1)$$

34 Where $\Delta\beta$ is the β difference across the current sheet, θ the magnetic shear angle, and
 35 $\frac{L_p}{d_i}$ is the pressure scale length in units of ion inertial length. At the dayside magnetopause,

36 near the magnetic equator where the X-line is expected to lie [Trattner et al., 2007], $\frac{L_p}{d_i}$
37 should be approximately equal to unity [Berchem & Russell, 1982]. With this assumption,
38 equation 1 becomes $\Delta\beta > 2 \tan\left(\frac{\theta}{2}\right)$. When this equation is satisfied, reconnection should
39 be suppressed by diamagnetic drift.

40 This process can explain why reconnection events are more often observed when the β
41 values in the adjacent magnetosheath are lower [Paschmann et al., 1986; Scurry & Russell,
42 1994; Phan & Paschmann, 1996; Trenchi et al., 2008]. Indeed, the magnetopause crossings
43 without reconnection signatures (non-reconnection events) recently examined by Phan et
44 al. [2013] generally satisfy the equation 1, while the opposite inequality usually held for
45 reconnection events. This process can also be important in the magnetopause of other
46 planets [Masters et al., 2012; DiBraccio et al., 2013].

47 In this paper, we analyzed a large dataset (207) of Double Star TC-1 magnetopause
48 crossings [Trenchi et al., 2008], which comprise both non-reconnection and reconnection
49 events. We verify the results of Phan et al. [2013], that the reconnection and non-
50 reconnection events are well-ordered by the Swisdak et al. [2010] relation. However, while
51 in previous studies the suppression condition was evaluated on the expectation that the
52 X-line was not too far away from the spacecraft, here we test the condition with the local
53 conditions at the X-line by separately considering a subset of events during which TC-1
54 observes a reversal in the jet direction, indicating that TC-1 was very close to the X-line.

55 Moreover, the main result of our paper is that by considering the latter subset, we are
56 able to demonstrate statistically that the motion of the X-line along the magnetopause
57 is controlled by the orientation of the guide-field. This verifies a second prediction made

58 by Swisdak et al. [2010]; in their simulation, when the local $\Delta\beta$ and θ are in the non-
 59 suppressed regime, the X-line moves in the direction of the diamagnetic drift of electrons.
 60 Since the pressure gradient at the dayside magnetopause is directed outward, this results
 61 in the motion of the X-line being controlled by the orientation of the guide field, i.e. by
 62 the B_Y GSM component of the IMF.

2. The Double Star TC-1 dataset

63 This Double Star TC-1 dataset, first examined to study the occurrence of reconnection
 64 at the magnetopause, comprises all the dayside magnetopause crossings observed by TC-1
 65 during the first year of the mission [Trenchi et al., 2008, 2009]. It is based on the plasma
 66 moments computed onboard from the Hot Ion Analyzer (HIA) [Rème et al., 2005] and
 67 magnetic field data measured by the Fluxgate Magnetometer (FGM) [Carr et al., 2005],
 68 both with four second time resolution.

69 In order to identify the reconnection events, we used the Walén relation and, as an
 70 example, we show an inbound magnetopause crossing in Figure 1. The first four panels
 71 display the ion density, velocity and temperatures and the magnetic field vector. For
 72 each data point in this time interval, we compared the observed velocity jump relative
 73 to a reference value in the magnetosheath ($V - V_{MSH}$) with the expected velocity jump
 74 predicted by the Walén relation (Equation (1) of Trenchi et al. [2008]). The magnetosheath
 75 reference period is indicated by yellow shading. Comparing these two vectors, we obtained
 76 the two parameters used to evaluate the agreement of the Walén relation: R_W as the ratio
 77 of their absolute values and Θ_W as their relative angle, shown in the last two panels of
 78 figure 1.

79 The Walén test is perfectly fulfilled when R_W equals unity and Θ_W equals 0° or 180° ,
 80 corresponding to the positive or negative signs of the Walén relation that at the dayside
 81 magnetopause correspond to observations northward or southward of the X-line. In this
 82 study we considered that the Walén relation is satisfied when $R_W > 0.4$ and $\Theta_W < 30^\circ$
 83 or $\Theta_W > 150^\circ$, for at least three consecutive data points, with average ion density larger
 84 than 1cm^{-3} [Trenchi et al., 2008]. This test indicates the presence of reconnection jets at
 85 the magnetopause or in the boundary layer. These criteria are meaningless when satisfied
 86 during magnetosheath intervals; therefore magnetosheath periods are excluded.

87 In this example, TC-1 crosses the magnetopause several times between 6:50 and 07:12
 88 UT, and later it has other encounters with the boundary layer. While in the first part of
 89 the event TC-1 detects northward and dawnward jets ($\Theta_W < 30^\circ$, blue shadings), after
 90 7:13 UT, it detects southward and duskward jets ($\Theta_W > 150^\circ$, pink shadings). This
 91 magnetopause crossing is classified as two-sided reconnection event, since TC-1 passes
 92 from northward to southward of the reconnection X-line, indicating it is very close to the
 93 spacecraft.

94 On the contrary, during other magnetopause crossings, called one-sided reconnection
 95 events, TC-1 detects reconnection jets that satisfy the Walén relation, but it remains on
 96 the same side of the X-line. Finally, during the non-reconnection events, no reconnection
 97 jet that satisfies the Walén relation is observed during the entire crossing. Overall, this
 98 database consists of 110 one-sided reconnection events, 33 two-sided reconnection events
 99 and 64 non-reconnection events, whose positions are shown in figure 2A, in the $Y - Z_{GSM}$
 100 plane.

3. Diamagnetic suppression of magnetic reconnection

101 For each of the TC-1 crossings, we identified a reference in the magnetosheath and
 102 another in the magnetosphere, both adjacent to the magnetopause, where we evaluated
 103 the average values of the ion pressure (as the trace of the pressure tensor measured by
 104 HIA) and the average magnetic field vectors. The plasma β in the Swisdak equation is
 105 the total β that includes both the ion and the electron pressures. However, the dayside
 106 magnetosheath is characterized by a large ion-to-electron temperature ratio ($\frac{T_i}{T_e}$), in the
 107 range 6-12 [Paschmann et al., 1993; Phan et al., 1994]. The same large ($\frac{T_i}{T_e}$) is also
 108 expected in the boundary layer, since it is related to the one in the adjacent magnetosheath
 109 [Lavraud et al., 2009]. Assuming quasi-neutrality, the ion and electron densities should be
 110 very similar. Therefore, it is expected that the ion pressure dominates over the electron
 111 pressure in these regions. For this reason, we evaluated the average total β from the ion
 112 pressure, assuming that the electron pressures are one eighth of the proton pressures on
 113 both sides of the magnetopause.

114 As expected, in the majority of cases (97%) the local β in the magnetosheath (MSH)
 115 is larger than the local β in the adjacent magnetosphere (MSPH). The few events with
 116 $\beta_{MSH} < \beta_{MSPH}$ (7/207), are characterized by a lower magnetic field magnitude in the
 117 magnetosphere with respect to the one in the magnetosheath, while the plasma pressure
 118 in the magnetosheath is always larger than the one in magnetosphere.

119 Figure 2B shows the scatter plot of the magnetic shear angle (θ) as a function of
 120 $|\Delta\beta|$ for the three families of events, where θ is the angle between the magnetosheath and
 121 magnetospheric reference magnetic fields. The black lines report the theoretical prediction

122 given by equation 1, in the hypothesis that $\frac{L_p}{d_i}$ is equal to 1 (continuous line) or 0.5
123 or 2 (dashed lines). These curves define the two regions of the $\theta - |\Delta\beta|$ plane where
124 reconnection should be suppressed (on the right), or where reconnection is possible since
125 it is not suppressed by the diamagnetic drift (on the left).

126 If we look at the non-reconnection events, they are spread across the suppressed and
127 non-suppressed regions. On the other hand, the majority of the reconnection events lie
128 in the region where reconnection is not suppressed, satisfying quite well the Swisdak
129 prediction. Considering the continuous line (1 ion inertial length thickness), 99/110 of
130 the one-sided reconnection events are in the non-suppressed region, i.e. 10% fall in the
131 suppressed region. This is a similar proportion to that found by Phan et al. [2013].
132 However, if we restrict our analysis to the two-sided reconnection events, for which we
133 can be confident that the spacecraft is near the X-line and hence the observed conditions
134 are more representative of the conditions at the X-line, all but one of the events (32/33)
135 is in the non-suppressed region. Therefore, the fraction of reconnection events in the
136 suppressed region is only 3% (1 event).

137 The presence of non-reconnection events in the region where reconnection should not
138 be suppressed by diamagnetic drift could indicate that another mechanism, for example
139 velocity shear [Cassak & Otto, 2011], turned off reconnection at the dayside magnetopause.
140 Alternatively, pulsed reconnection may have been occurring [Trattner et al., 2015], causing
141 the reconnection jet to be missed when TC-1 crossed the magnetopause.

142 On the other hand, the one-sided reconnection events in the suppressed region are
143 not necessary at odds with the Swisdak predictions: these reconnection events could

144 be observed several Earth radii away from the X-line. Taking into account the magnetic
 145 shear variations along the magnetopause caused by magnetic field draping, the local shear
 146 obtained for these one-sided events could differ significantly from the shear at the X-line.
 147 Moreover, according to the maximum shear model [Trattner et al., 2007], the X-line follows
 148 the position of the local maximum of the shear angle at each local time. In this case, any
 149 displacement from the X-line would result in the underestimation of shear angle at the
 150 X-line, which could explain the local $\theta - |\Delta\beta|$ values in the suppressed region.

151 Another feature that can be noted in figure 2B is that, while several one-sided recon-
 152 nection events have very low $|\Delta\beta|$, the two-sided reconnection events have all $|\Delta\beta| > 0.1$,
 153 being more concentrated near the theoretical suppression condition of Swisdak. According
 154 to the diamagnetic drift effect, the X-line velocity increases as the suppression condition
 155 is approached, and, a larger X-line velocity could explain the passage of the spacecraft
 156 from one to the other side of the X-line during these two-sided events. This suggests that
 157 the diamagnetic drift has a role for the motion of the X-line when reconnection is not
 158 suppressed. In the following section, we use a subset of two-sided reconnection events to
 159 study the X-line motion along the magnetopause.

4. The motion of the X-line along the dayside magnetopause

160 According to the Swisdak simulations, the X-line should move along the current sheet
 161 in the direction of the diamagnetic drift of the electrons. The X-line velocity with respect
 162 to the ion rest frame is given by the sum of the ion and electron diamagnetic drift:

$$V_{XLdrift} = c \frac{\nabla p_i \times \vec{B}_g}{|q_i| n_i B_g^2} + c \frac{\nabla p_e \times \vec{B}_g}{|q_e| n_e B_g^2} \quad (2)$$

163 where c is the speed of light, \vec{B}_g is the guide field at the center of the current sheet, while
 164 p_i and p_e , q_i and q_e , n_i and n_e are the pressures, charges and densities of ions and electrons,
 165 respectively. At the dayside magnetopause, where the pressure gradient is outward along
 166 the magnetopause normal, the direction of the X-line motion is related to the orientation
 167 of the guide field, which is mainly determined by the B_Y component of the IMF. Therefore
 168 the X-line is expected to move northward/southward for duskward/dawnward guide fields
 169 respectively.

170 The guide field can be evaluated as the projection of the magnetosheath or magneto-
 171 spheric field along the X-line. For the two-sided reconnection events, we evaluated the
 172 orientation of the X-line predicted by the component merging model [Sonnerup, 1974;
 173 Gonzales & Mozer, 1974] from the magnetosheath and magnetospheric fields, which are
 174 likely to be similar to the fields at the reconnection site. Here we introduce a local refer-
 175 ence frame, with \widehat{N} along the Fairfield magnetopause normal [Fairfield, 1971], \widehat{XL} along
 176 the X-line orientation with a positive Y_{GSM} component and \widehat{RC} (representing the recon-
 177 necting component), perpendicular to these vectors, with a positive Z_{GSM} component (see
 178 figure 3). The X-line orientation is obtained as perpendicular to $\vec{B}_{MSH} - \vec{B}_{MSPH}$, where
 179 \vec{B}_{MSH} and \vec{B}_{MSPH} are the projections in the plane perpendicular to the Fairfield normal
 180 of the magnetosheath and magnetospheric fields, respectively.

181 For several two-sided reconnection events, a single passage from northward to southward
 182 jets, or vice versa, is observed during the entire crossing, such as in the example shown in
 183 figure 1. In these single passage events we can make the simplifying assumption that the
 184 X-line velocity does not change direction during the event. On the contrary, other two-

185 sided events are characterized by multiple passages between northward and southward
 186 jets. This could be due to the presence of multiple X-lines, which could eventually move
 187 in the same direction, or alternatively to a reversal of the X-line motion. In the former
 188 case, the formation of FTEs between the multiple X-lines is expected [Lee & Fu, 1985;
 189 Raeder, 2006; Trenchi et al., 2011; Fear et al., 2012a, b].

190 In figure 2B, the black bars over the cyan dots indicate the two-sided single passage
 191 events. It is interesting to note that all the two-sided events with low magnetic shear
 192 ($\theta < 90^\circ$) are characterized by a single passage. In figure 4A we report the distribution of
 193 the magnitude of \vec{B}_g for single passage and multiple passage events. In agreement with
 194 their lower magnetic shear, the single passage events have a much stronger guide field
 195 compared with the multiple passage events. The average values are $|\vec{B}_g| = 26 \pm 15nT$
 196 and $|\vec{B}_g| = 6 \pm 5nT$ for the single passage and multiple passage events, respectively.
 197 According to equation 2, a higher guide field would produce a larger X-line velocity,
 198 which could be responsible for the clear constant motion of the X-line in one direction
 199 during these single passage events.

200 The direction of the X-line motion can be easily inferred for the single passage events
 201 from the order in which northward and southward reconnection jets are observed. When
 202 first northward and then southward reconnection jets are detected, the X-line is moving
 203 northward with respect to the spacecraft, while it is moving southward when the order of
 204 the reconnection jets is the opposite. In figure 4B, B_g as a function of the order in which
 205 the jets are detected for the single passage events is reported. The blue dots indicate

206 the northward-southward events (N-S), while the red dots are the southward-northward
207 events (S-N).

208 Our observations show a good agreement with the diamagnetic motion of the X-line: all
209 the S-N events have a negative B_g , and all but one of the N-S events have a positive B_g .
210 The only N-S event with a negative guide field still has a B_g very close to zero ($-0.4nT$).
211 These observations suggest therefore that the diamagnetic drift has a role in the X-line
212 motion along the magnetopause when the local conditions are not in the suppressed region,
213 as predicted by the simulations of Swisdak et al. [2003]. We also verified that using other
214 X-line models [Moore et al., 2002; Swisdak & Drake, 2007; Borovsky, 2013] the orientation
215 of the guide field B_Y component do not change. Therefore, the choice of a different X-line
216 model would not change our findings.

217 The other mechanism that could be responsible for the X-line motion is the convection
218 from the adjacent magnetosheath. Indeed, a recent study found that during a reconnection
219 event at high latitude characterized by super-Alfvenic magnetosheath velocity, the X-line
220 was moving tailward convected by the magnetosheath velocity [Wilder et al., 2014]. We
221 therefore evaluated the component of the magnetosheath velocity perpendicular to the
222 X-line (V_{MSHRC}), which is the component that could convect the X-line. If the X-line
223 motion is related to the magnetosheath convection, since the RC axis has a positive Z_{GSM}
224 component, N-S events should be associated with positive V_{MSHRC} while S-N events with
225 negative V_{MSHRC} . We also estimated the X-line diamagnetic drift velocity predicted by
226 the Swisdak simulation with equation 2). As for the suppression condition, we assumed

227 that the electron pressures are one eighth of the proton pressures on both sides of the
 228 magnetopause and $\frac{L_p}{d_i}$ is equal to 1. The X-line velocity is therefore obtained as:

$$V_{XLdrift} = c \frac{9}{8} \frac{(p_{MSH} - p_{MSPH}) B_g}{d_i | q_i | n_i B_g^2} \hat{R}C \quad (3)$$

229 where p_{MSH} and p_{MSPH} are the average proton pressures in magnetosheath and magne-
 230 tospheric reference, respectively. While these assumptions can certainly introduce errors
 231 in the values of $V_{XLdrift}$, we believe that it can not change its sign, since outward pressure
 232 gradient at the magnetopause implies that $p_{MSH} > p_{MSPH}$.

233 In figure 4C, $V_{XLdrift}$ as a function of V_{MSHRC} is reported. Blue and red dots refer
 234 to N-S and S-N events, for which the velocity of the X-line is northward and southward
 235 respectively. $V_{XLdrift}$ better separates the N-S from the S-N events. Indeed, all the S-N
 236 events are associated with negative $V_{XLdrift}$ and all but one of the N-S events are associated
 237 with positive $V_{XLdrift}$. On the contrary, five of the N-S events are observed during negative
 238 V_{MSHRC} , contrary to expectation according to the magnetosheath convection. Therefore,
 239 it seems that the velocity of the adjacent magnetosheath does not affect the motion of the
 240 X-line at the dayside magnetopause. However it is interesting to note that the only event
 241 not in agreement with the diamagnetic drift, the only N-S event with negative $V_{XLdrift}$,
 242 is the only event with V_{MSHRC} larger than Alfvén magnetosheath velocity. In this case,
 243 the magnetosheath convection hypothesis is in agreement with the order of the jets.

5. Summary and Conclusions

244 During component reconnection, the diamagnetic drift of ions and electrons causes a
 245 motion of the X-line along the dayside magnetopause, which is proportional to the local

246 pressure gradient and to the intensity of the guide field at the X-line [Swisdak et al., 2003].

247 If this X-line velocity exceeds the local Alfvén speed, reconnection is suppressed.

248 In order to investigate the effects of diamagnetic drift, we analysed a large dataset of
249 Double Star TC-1 magnetopause crossings (207) which includes both reconnection events
250 and magnetopause crossings without reconnection signatures. The reconnection events
251 were divided into two categories, one where the distance of the spacecraft from the X-line
252 is unknown (one-sided events, can be also several R_E from the X-line), the other one where
253 TC-1 explores both sides of the X-line, being probably very close to the reconnection site
254 (two-sided events). This latter category allows us to test the suppression condition with
255 the local conditions at the X-line.

256 We found that most of the reconnection events were observed in the regime where recon-
257 nection is not predicted to be suppressed by diamagnetic drift. Moreover, the agreement
258 with the suppression condition further increased when the spacecraft was near the X-line
259 (97%, or 32/33 of the two-sided events in the non-suppressed region) with respect to the
260 one-sided events (90% in the non-suppressed region). The fact that the local conditions
261 at the X-line show such a good agreement with the suppression condition, confirms that
262 the diamagnetic drift is able to turn off reconnection at the dayside magnetopause.

263 For several two-sided events, we also determined the direction of the X-line motion with
264 respect to the spacecraft, from the order in which northward and southward reconnection
265 jets were detected. With these events, we tested if the X-line motion is related to the
266 diamagnetic drift, which should move the X-line in the direction of the electron drift even
267 when reconnection is not suppressed [Swisdak et al., 2003]. At the magnetopause, where

268 the pressure gradient is outward, the direction of the X-line motion should be related
269 to the orientation of the guide field, which is principally determined by the IMF B_Y
270 component.

271 We found that the direction of the X-line motion is in agreement with the velocity
272 predicted by the diamagnetic drift for all but one of these events (9/10), which are all
273 characterized by a non-negligible guide field. The only event not in agreement with the
274 diamagnetic drift prediction has instead a very small guide field, which results in a small
275 X-line velocity. On the contrary, the convection hypothesis is not in agreement with the
276 observations for half of these events. This suggests that, during component reconnection,
277 the X-line has always a motion along the magnetopause under the effect of diamagnetic
278 drift. This X-line motion, not considered by the present models that predict the X-line
279 location, can cause a non-stationary reconnection even for stable solar wind conditions.

280 **Acknowledgments.** L.T. is currently supported by STFC Ernest Rutherford
281 Grant ST/L002809/1, and R.F. is supported by STFC Ernest Rutherford Fellow-
282 ship ST/K004298/1. Double Star data are available via Cluster Science Archive
283 (<http://www.cosmos.esa.int/web/csa>). L.T. thanks M. Hesse and G. Pallochia for the
284 useful discussions.

References

- 285 Berchem, J., & Russell, C. T. 1982, The thickness of the magnetopause current layer -
286 ISEE 1 and 2 observations, *J. Geophys. Res.*, , 87, 2108
- 287 Borovsky, J. E. 2013, *Journal of Geophysical Research (Space Physics)*, 118, 2113

- 288 Carr, C., , Brown, P., Zhang, T. L., Gloag, J., Horbury, T., Lucek, E., Magnes, W.,
289 O'Brien, H., Oddy, T., Auster, U., Austin, P., Aydogar, O., Balogh, A., Baumjohann,
290 W., Beek, T., Eichelberger, H., Fornacon, K.-H., Georgescu, E., Glassmeier, K.-H.,
291 Ludlam, M., Nakamura, R., and Richter, I (2005). The Double Star magnetic field
292 investigation: instrument design, performance and highlights of the first year's of obser-
293 vations, *Ann. Geophys.*, *23*, 2713-2732, 2005.
- 294 Cassak, P. A., & Otto, A. 2011, *Physics of Plasmas*, *18*, 074501.
- 295 Dibraccio, G. A., Slavin, J. A., Boardsen, S. A., et al. 2013, *Journal of Geophysical*
296 *Research (Space Physics)*, *118*, 997.
- 297 Fairfield D. H. (1971), Average and unusual locations of the Earth's magnetopause and
298 bow shock, *J. Geophys. Res.*, *76*, 6700.
- 299 Fear, R. C., M. Palmroth and S. E. Milan, Seasonal and clock angle control of the location
300 of flux transfer event signatures at the magnetopause, *J. Geophys. Res.*, *117*, A04202,
301 doi:10.1029/2011JA017235, 2012
- 302 Fear, R. C., S. E. Milan and K. Oksavik, Determining the axial direction of high-shear
303 flux transfer events: Implications for models of FTE structure, *J. Geophys. Res.*, *117*,
304 A09220, doi:10.1029/2012JA017831, 2012
- 305 Gonzales, W. D. and F. S. Mozer (1974), A quantitative model from the potential resulting
306 from reconnection with an arbitrary interplanetary magnetic field, *J. Geophys. Res.*, ,
307 *79*,4186.
- 308 Lavraud, B., Borovsky, J. E., Génot, V., et al. 2009, Tracing solar wind plasma entry into
309 the magnetosphere using ion-to-electron temperature ratio, *Geophys. Res. Lett.*, , *36*,

310 L18109

311 Lee, L. C. and Z. F. Fu (1985), A theory of magnetic flux transfer at the Earth's magne-
312 topause, *Geophys. Res. Lett.*, *12*, No. 2, pages 105-108.

313 Masters, A., Eastwood, J. P., Swisdak, M., et al. 2012, *Geophys. Res. Lett.*, , 39, L08103.

314 Moore, T. E., Fok, M.-C., & Chandler, M. O. 2002, *Journal of Geophysical Research*
315 (Space Physics), *107*, 1332

316 Paschmann G., Baumjohann W., Sckopke N., Papamastorakis I., Carlson, C. W., Son-
317 nerup B. U. Ö. and Lühr H. (1986), The magnetopause for large magnetic shear -
318 AMPTE/IRM observations, *J. Geophys. Res.*, *91*, 11,099-11,115.

319 Paschmann, G., Baumjohann, W., Sckopke, N., Phan, T.-D., & Luehr, H. Structure of
320 the dayside magnetopause for low magnetic shear, 1993, *J. Geophys. Res.*, , 98, 13409

321 Phan, T.-D., Paschmann, G., Baumjohann, W., Sckopke, N., & Luehr, H. 1994, The mag-
322 netosheath region adjacent to the dayside magnetopause: AMPTE/IRM observations,
323 *J. Geophys. Res.*, , 99, 121

324 Phan, T.D. and Paschmann, G., Ö. Sonnerup, (1996), Low-latitude dayside magnetopause
325 and boundary layer for high magnetic shear 2. Occurrence of magnetic reconnection in
326 *J. Geophys. Res.*, *101*, 7817-7828, 1996.

327 Phan, T. D., Paschmann, G., Gosling, J. T., et al. 2013, The dependence of magnetic re-
328 connection on plasma and magnetic shear: Evidence from magnetopause observations,
329 *Geophys. Res. Lett.*, , 40, 11

330 Raeder, J., (2006), Flux Transfer Events: 1. generation mechanism for strong southward
331 IMF, *Ann. Geophys.*, *24*, 381-392,2006.

- 332 Rème, H. , Dandouras, I., Aoustin, C., Bosqued, J. M., Sauvaud, J. A., Vallat, C.,
333 Escoubet, P., Cao, J. B., Shi, J., Bavassano-Cattaneo, M. B., Parks, G. K., Carlson, C.
334 W., Pu, Z., Klecker, B., Moebius, E., Kistler, L., Korth, A., Lundin, R., and the HIA
335 team, (2005), The HIA instrument on board the Tan Ce 1 Double Star near-equatorial
336 spacecraft and its first results, *Ann. Geophys.*, *23*, 2757-2774, 2005.
- 337 Scurry, L. and Russell, C.T., Gosling, J.T., (1994), A statistical study of accelerated flow
338 events at the dayside magnetopause, in *J. Geophys. Res.*, *99*, 14,815-14,829, 1994.
- 339 Sonnerup, B. U. Ö. (1974), The reconnecting magnetosphere, in *Magnetospheric Physics*,
340 edited by B. M. McCormac, p. 23, D. Reidel, Dordrecht-Holland.
- 341 Swisdak, M., Rogers, B. N., Drake, J. F., & Shay, M. A. 2003, Diamagnetic suppression
342 of component magnetic reconnection at the magnetopause *J. Geophys. Res.*, , 108, 1218
- 343 Swisdak, M., & Drake, J. F. 2007, *Geophys. Res. Lett.*, , 34, L11106
- 344 Swisdak, M., Opher, M., Drake, J. F., & Alouani Bibi, F. 2010, The Vector Direction of
345 the Interstellar Magnetic Field Outside the Heliosphere *Astrophys. J.*, , 710, 1769
- 346 Trattner, K. J., Mulcock, J. S., Petrinec, S. M., & Fuselier, S. A. 2007, Probing the bound-
347 ary between antiparallel and component reconnection during southward interplanetary
348 magnetic field conditions *J. Geophys. Res.*, , 112, A08210
- 349 Trattner, K. J., Onsager, T. G., Petrinec, S. M., & Fuselier, S. A. 2015, Journal of
350 Geophysical Research (Space Physics), 120, 1684.
- 351 Trenchi, L., M. F. Marcucci, G. Pallochia, G. Consolini, M. B. Bavassano Cattaneo, A.
352 M. Di Lellis, H. Rème, L. Kistler, C. M. Carr, and J. B. Cao 2008, Occurrence of
353 reconnection jets at the dayside magnetopause: Double Star observations, *J. Geophys.*

354 *Res.*, 113, A07S10, doi:10.1029/2007JA012774.

355 Trenchi, L., Marcucci, M. F., Pallocchia, G., et al. 2009, Magnetic reconnection at the
356 dayside magnetopause with Double Star Tc1 data. *Memorie della Società Astronomica*
357 *Italiana*, 80, 287

358 Trenchi, L., Marcucci, M. F., Rème, H., Carr, C. M., & Cao, J. B. 2011, TC-1 observations
359 of a flux rope: Generation by multiple X-line reconnection. *Journal of Geophysical*
360 *Research (Space Physics)*, 116, A05202

361 Wilder, F. D., Eriksson, S., Trattner, K. J., et al. 2014, Observation of a retreating X-line
362 and magnetic islands poleward of the cusp during northward interplanetary magnetic
363 field conditions, *Journal of Geophysical Research (Space Physics)*, 119, 9643

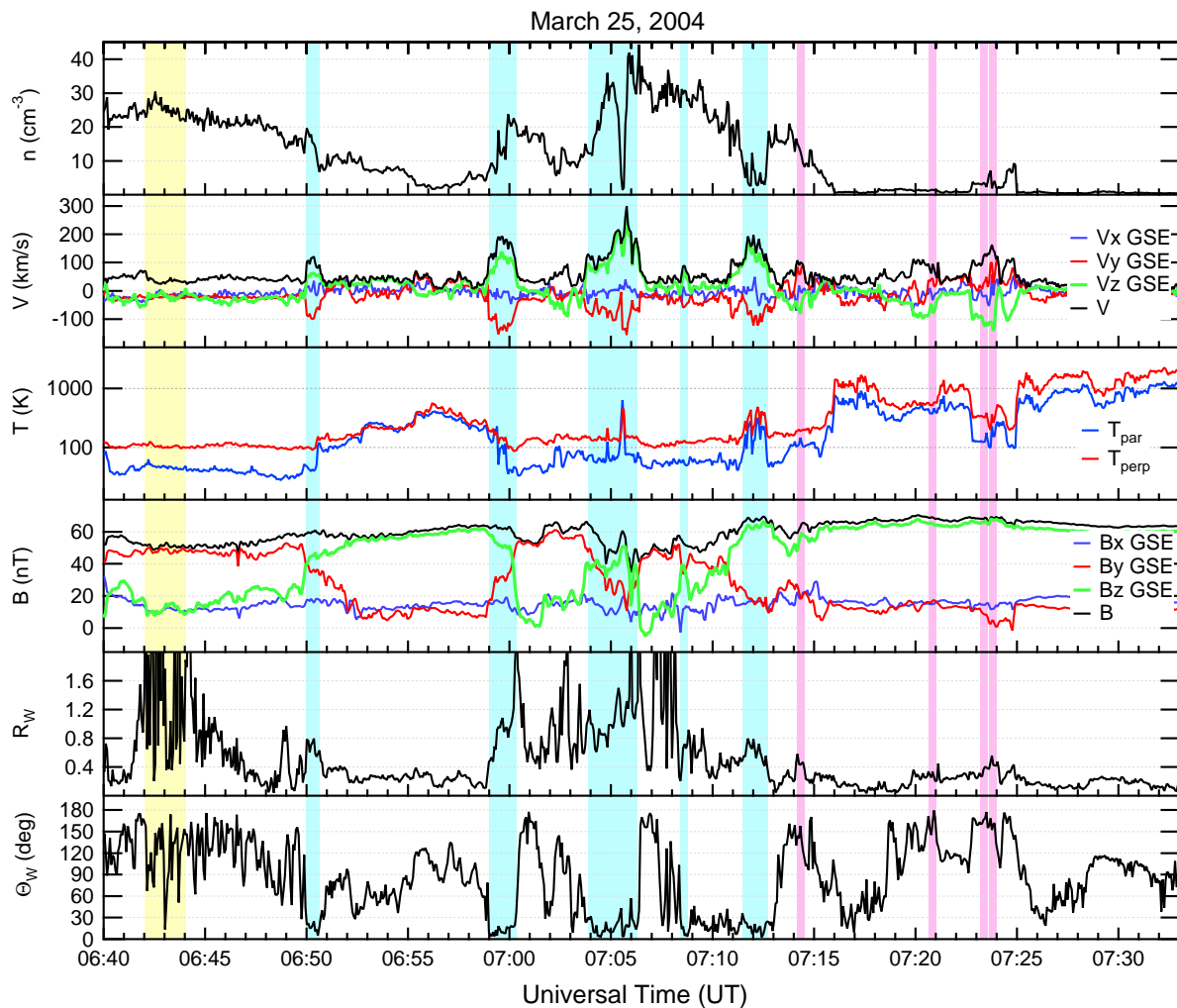


Figure 1. An example of magnetopause crossing with reconnection jets. In the top four panels the ion density, velocity, temperatures and the magnetic field vector. The last two panels show the parameters used to evaluate the agreement of the Walén test, that is perfectly fulfilled when R_W equals unity and Θ_W equals 0° or 180° , corresponding to observations northward or southward of the X-line. In this event TC-1 explores both sides of the X-line, observing first northward and then southward reconnection jets, therefore it is classified as a two-sided event.

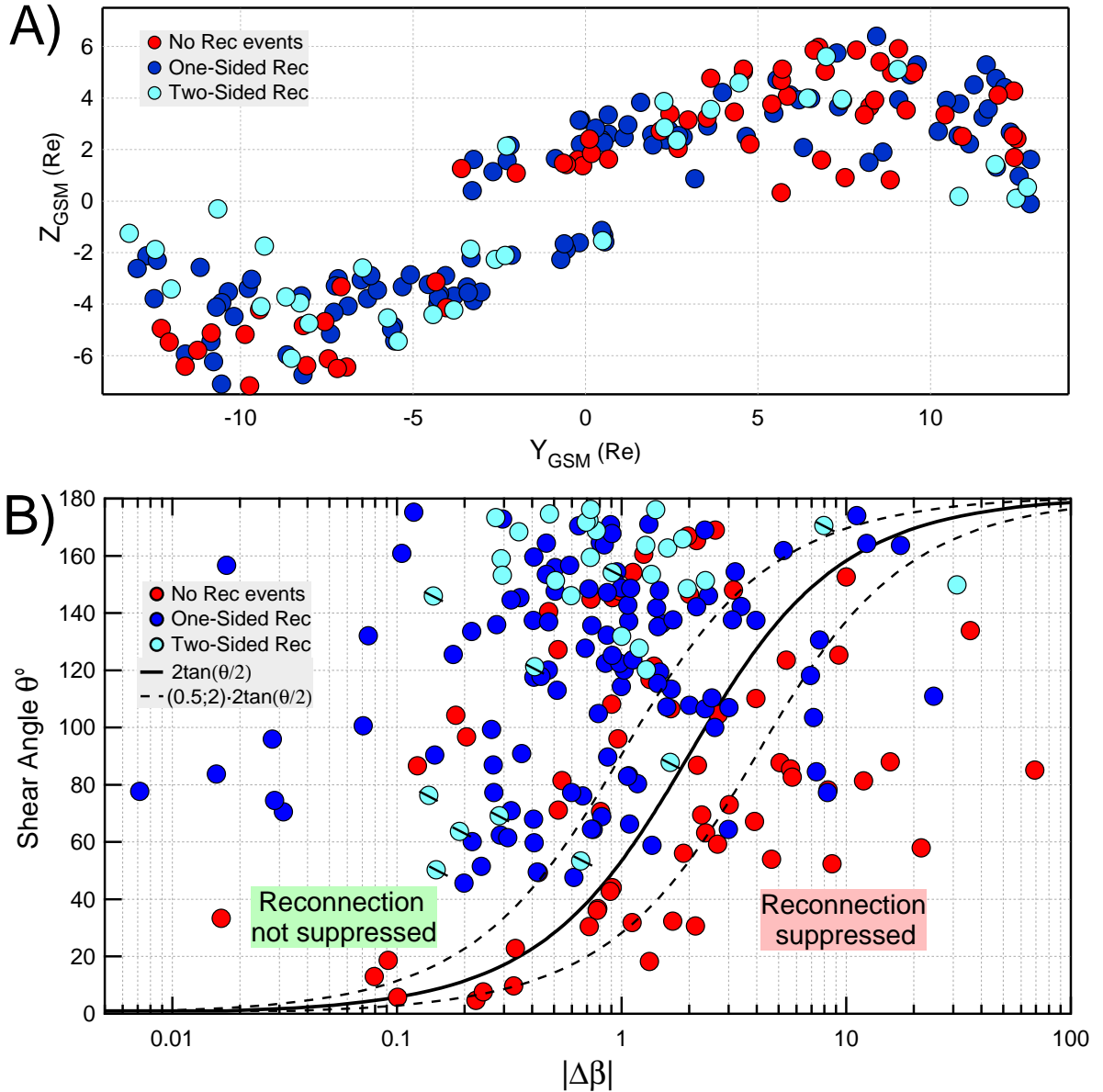


Figure 2. Panel A). The positions of the non-reconnection events (red dots), one-sided reconnection events (blue dots) and two-sided reconnection events (cyan dots) in the $Y - Z_{GSM}$ plane.

Panel B). The magnetic shear angle (θ) as a function of $|\Delta\beta|$ for the non-reconnection events (red dots), one-sided reconnection events (blue dots) and two-sided reconnection events (cyan dots). The black lines are the prediction for the diamagnetic suppression of reconnection (equation 1), when $\frac{L_p}{d_i}$ is equal to 1 (continuous line) or 0.5 or 2 (dashed lines). On the right of these curves, reconnection should be suppressed by diamagnetic drift effect, while on the left it should not be suppressed.

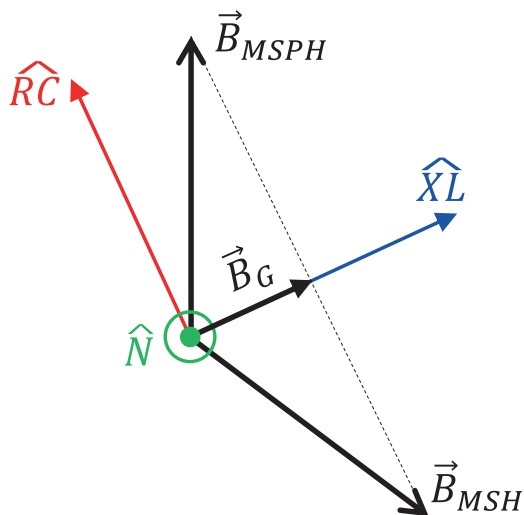


Figure 3. A scheme of the local X-line reference used to evaluate the guide field component (\vec{B}_g) for the two-sided reconnection events.

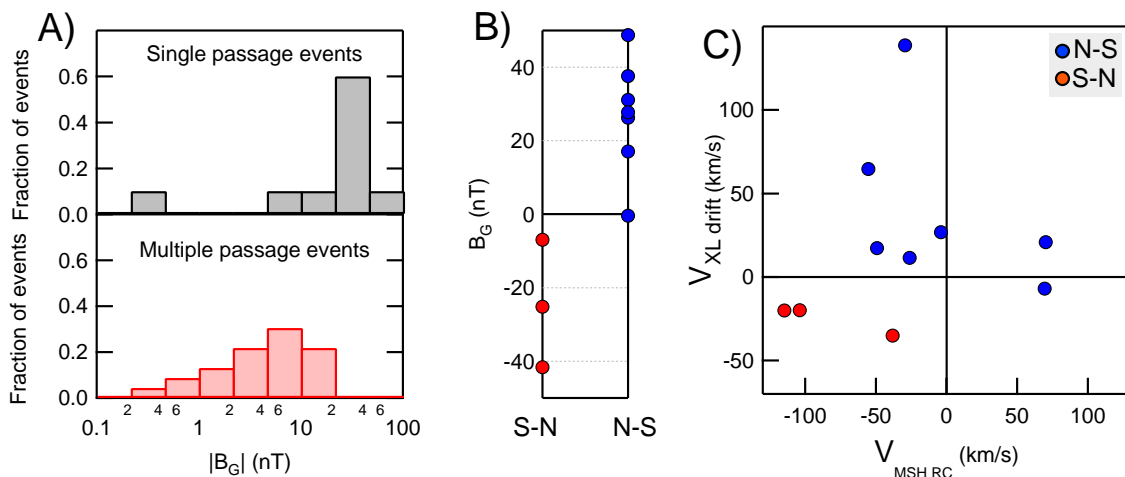


Figure 4. Panel A). The histograms of the magnitude of the guide field component for single passage and multiple passage events.

Panel B). B_g as a function of the order in which the jets are detected. Panel C). The diamagnetic drift velocity of the X-line as a function of the velocity of the adjacent magnetosheath perpendicular to the X-line. Blue and red dots indicate N-S and S-N events, for which the observed X-line velocity is northward and southward, respectively.